Sensors and Materials, Vol. 15, No. 2 (2003) 067–081
MYU Tokyo

S & M 0510

Modelling of Anisotropic Etching of Silicon: Anomalies due to Facet Boundary Effects

Ziyad Elalamy, Leslie M. Landsberger*, Mojtaba Kahrizi, Anand Pandy, Irina Stateikina and Sébastien Michel†

Department of Electrical and Computer Engineering,
Concordia University, Montréal, QC, Canada H3G-1M8

(Received September 30, 2002; accepted February 21, 2003)

Key words: anisotropic etching of silicon, crystal-based modelling anomalies

In the crystal-based modelling of wet anisotropic etching of silicon, one begins with the hypothesis that the etch rate in a specific etchant composition at a given temperature should depend only on the crystal features of the surface exposed to the etchant. However, analysis of experimental data reveals interesting features which contradict this hypothesis. A given crystal surface having particular crystal indices, under a particular set of etchant conditions (composition, temperature), may exhibit significant differences in etch rate. These anomalies are hypothesized to be driven by effects due to the boundaries of the under-etched facets.

1. Introduction

Wet anisotropic etching of silicon is a widespread micro-fabrication technique used to create 3-D shapes in bulk silicon. Many microsystems fabrication processes include such an etch to form cavities or release suspended membranes or microstructures. The planes selected are usually {111} or {100} due to their relatively slow etch rates, predictable inclination angles, and surface flatness. Other planes such as fast-etch planes, or other intermediate planes, are less often used or studied. Several research groups have systematically experimentally studied anisotropic etching of silicon[1–12] and addressed the modelling of etch mechanisms.[2, 5–7, 12–17] Yet a comprehensive theoretical understanding of etch mechanisms and phenomena remains difficult.

* Corresponding author, e-mail address: leslie@ece.concordia.ca
† Current address: Dalsa Semiconductor, 18, boul. de l'Aéroport, Bromont, Québec, Canada, Sebastien.Michel@dalsasemi.com

In the modelling of wet anisotropic etching of silicon, a common starting point is the hypothesis that the etch rate in a specific etchant composition at a given temperature should depend only on the crystal features of the surface being presented to the etchant.[14] However, such crystal features are not always etched at the same rate, depending on such factors as geometrical attitude and adjacent facets.[13,15–18] Further, analysis of a body of experimental data[1,13,16–18] reveals interesting features which contradict the crystal-feature-based hypothesis in several specific ways.

With a view to a more comprehensive modelling of the technique, this work (a) introduces an analytical technique by which to predict the results of an under-etch experiment which would occur if the same crystal features are always etched at the same rate, and (b) presents experimental observations (anomalies) which demonstrate that the above hypothesis often does not apply.

2. Experimental Procedure

Six (6) {100} and six (6) {110} oxide-covered silicon samples, wagon-wheel patterned, were immersed simultaneously in fresh 19wt.% and 25wt.% TMAH. Half of the wagon-wheel layout used for Si{100} is shown in Fig. 1. A similar pattern was also designed for Si{110}. The solution was heavily stirred and the temperature was adjusted to 80°C. A reflux condenser was used to keep the TMAH concentration constant. After time periods of 10 min, 25 min, 50 min, 1 h 30 min, 3 h, and 5 h (measured from the beginning of the experiment), one sample of each orientation was removed from the etching solution.

2.1 *Measurements*

Optical measurements were performed to measure the under-etch rate (UER), the bottom width, and the bottom-surface etch rate (see Fig. 2) at each spoke of the wagon-wheel. Spokes are regularly spaced at 1°, 2°, or 4° (according to the etching time). The deviation angle (δ) measures the positioning of the spokes from a reference line indicating vertical {100} planes. SEM images enabled the characterization of under-etched facets (lengths and inclination angles (α)).

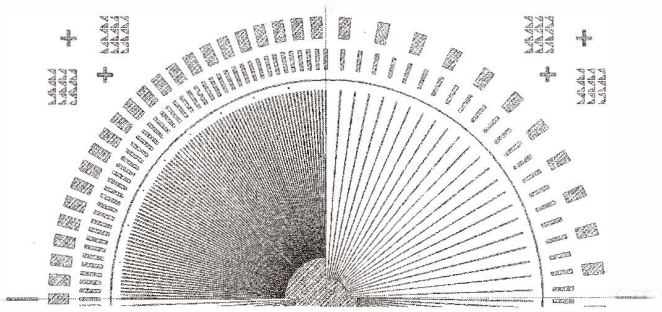

Fig. 1. Half of the wagon-wheel layout designed for Si{100}.

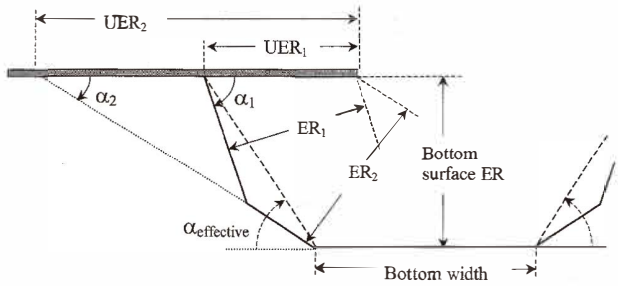

Fig. 2. Schematic cross section of a single spoke at a given deviation angle (δ) involving two under-etched facets.[16]

2.2 *Stirring effects*

Figure 3 shows the results of wagon-wheel under-etch rate measurements on Si{100} etched in unstirred TMAH. The unstirred curves in Fig. 3 are globally symmetric around δ=0° (which is normal due to the symmetry of Si{100}), but upon closer inspection, one sees that the curves are irregular and asymmetric.

For better clarity, curves from the two sides of Fig. 3 (the 25 min and 6 h data) are folded horizontally around δ=0° and presented in Fig. 4. Dotted lines in Fig. 4 correspond to measurements on spokes at deviation angles $-45° \leq \delta \leq 0°$ (the left side of Fig. 3), symmetrically transposed for comparison with solid lines that correspond to measurements at $0° \leq \delta \leq 45°$ (the right side of Fig. 3). The fact that in Fig. 4 solid lines and dotted lines do not coincide demonstrates that the corresponding curves in Fig. 3 are actually not symmetric. In contrast, Fig. 5 shows folded under-etch rate curves obtained from vigorously stirred experiments using a 6 cm magnetic stirrer at about 500 rpm. Solid lines and dotted lines coincide satisfyingly, which suggests that vigorous stirring is effective against the anomalies observed without stirring.

3. Etching Model

3.1 *P-based and K-based planes*

The etching model assumes that two families of planes compose (approximately) all facets of an under-etch profile (such as in Fig. 2). The first family of planes is defined by (hhl) Miller indices, where "h" is a high-numbered index while "l" is a low-numbered index. (hhl) planes are denoted "P-based planes" and have their surfaces ideally microscopically covered by zigzag chains (periodic bond chains – PBCs[19]) of atoms, each having one dangling bond. The second family of planes is defined by (hll) Miller indices. Planes of the second family are denoted "K-based planes" and have their surfaces ideally covered by rows of kinks. A kink is an atom having two dangling bonds. Each of the P-based and K-based series of planes evolves from a {111} plane by rotation (of an angle θ) around an axis oriented in a <110> direction. For example, (111), (221), (331), and (110) planes belong to the same P-based series, and $(1\bar{1}1)$, $(3\bar{1}1)$, $(4\bar{1}1)$, and (100) belong to the same K-based series. P-based series (or K-based series) are described (see Fig. 6) by

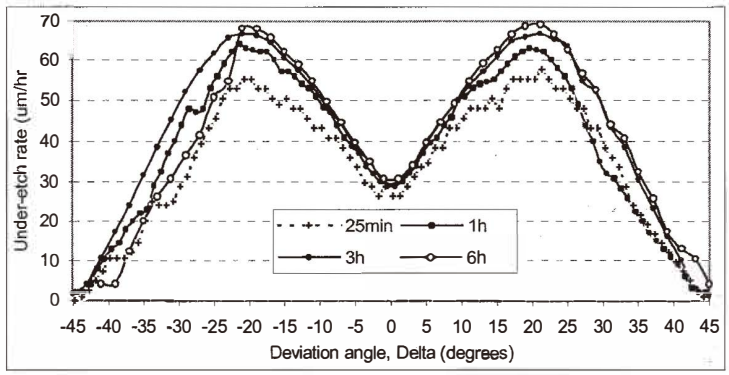

Fig. 3. Under-etch rate evolution with time of Si{100} etched in unstirred 25wt.% TMAH.

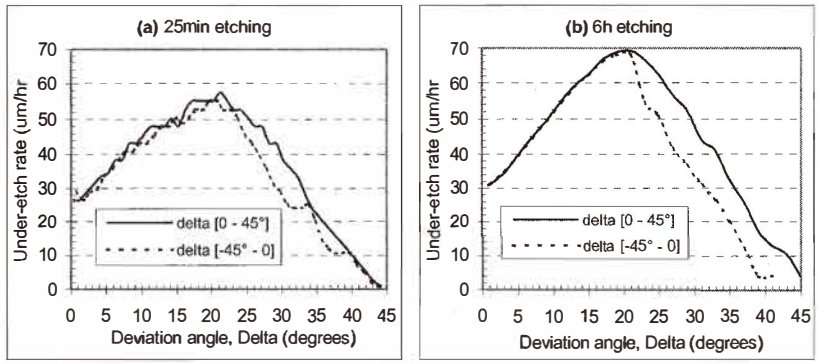

Fig. 4. Examples of irregular and poorly symmetric curves for unstirred Si{100} 25wt% TMAH. The 25 min (a) and 6 h (b) etching curves are folded around δ=0°.

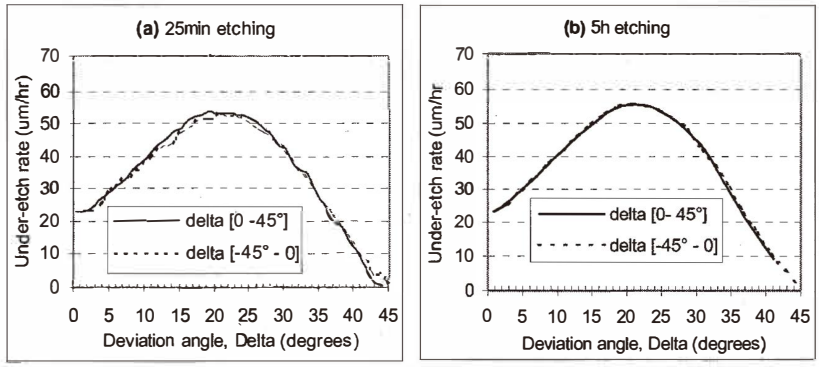

Fig. 5. Examples of regular and symmetric curves for stirred Si{100} 25wt% TMAH. The 25 min (a) and 5 h (b) etching curves are folded around δ=0°.

angles of rotation θ_p (or θ_k) with respect to a given {111}-family plane.

The inclination angles (α) of P-based and K-based series for Si{100} and Si{110} are summarized in Fig. 7 and Fig. 8, respectively. To illustrate the use of Fig. 7 (or Fig. 8), let us consider an under-etching experiment on Si{100}, the mask edge being positioned at

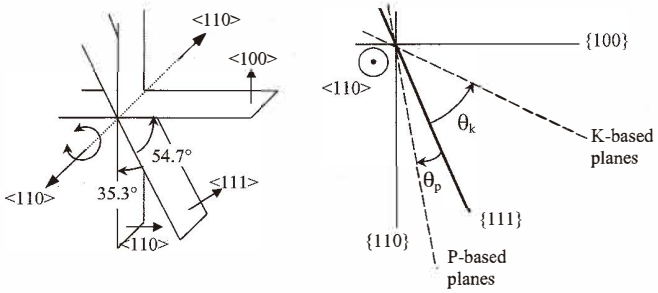

Fig. 6. Rotation angles from {111} : θ_p and θ_k.[16]

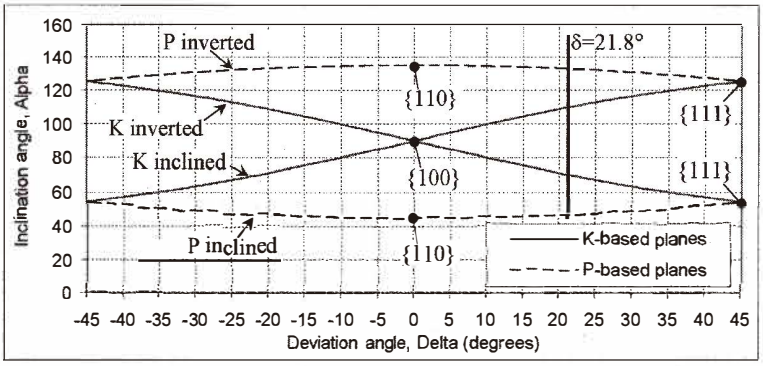

Fig. 7. Theoretical P-based and K-based planes' inclination angles (α) versus mask edge deviation angle (δ) for Si{100}.[16]

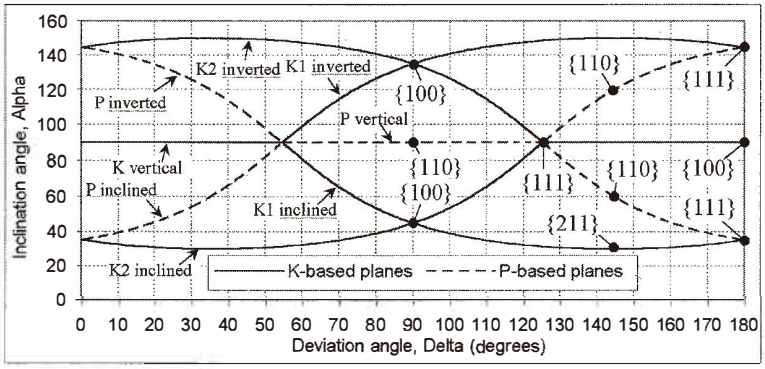

Fig. 8. Theoretical P-based and K-based planes' inclination angles (α) versus mask edge deviation angle (δ) for Si{110}.[16]

23.2° from the wafer flat, e.g. δ = (45°–23.2°) = 21.8°. At this δ, we find that four different planes (two P-based, two K-based)† may be involved in shaping the under-etch profile. The inclination angles of these planes are 47.12°, 69.63°, 110.37°, and 132.88°, respectively.

Actual experimental under-etched inclination angles should be observed and compared with these theoretical inclination angles. If they match, then one can conclude (forced by basic geometry of the silicon crystal structure) that the actual facets are indeed P-based or K-based facets. Notice in Fig. 7 (corresponding to Si{100}), that a maximum of four facets may compose the under-etch profile, while in Fig. 8 (corresponding to Si{110}), up to five facets may appear. Notice also the lowest possible inclination angle (α) among all facets is 45° for Si{100} (reached at δ = 0° by a {110} facet), while in the case of Si{110}, the lowest possible inclination angle (α) among all facets is 30° (reached at δ = 35.26° or 144.74° by a {211} facet).

3.2 *P-based and K-based canonical curves*

The etching model based on the P-based and K-based families of planes may be used to predict under-etch rates (Fig. 10(a)) and under-etch profiles (Fig. 11). To perform such predictions, it is required to previously estimate the etching rates of P-based and K-based series. These estimates are referred to as "canonical curves". Examples of such estimated canonical curves for 25wt% and 19wt% TMAH are presented in Fig. 9 with respect to the deviation angles θ_p and θ_k (angles defined in Fig. 6).

3.3 *Under-etch rate predictions*

Based on the canonical curves of P-based and K-based planes (Fig. 9), one can obtain the under-etch rates (example of Si{110} 25wt% TMAH, shown in Fig. 10(a)), which would correspond to the various P-based and K-based series variations as a function of δ. Figure 10(a) helps to predict the actual under-etch rate by following the curve composed of the slowest under-etching portions. It can be seen indeed that the shape of the experimental data in Fig. 10(b) follows this model closely, but not exactly.

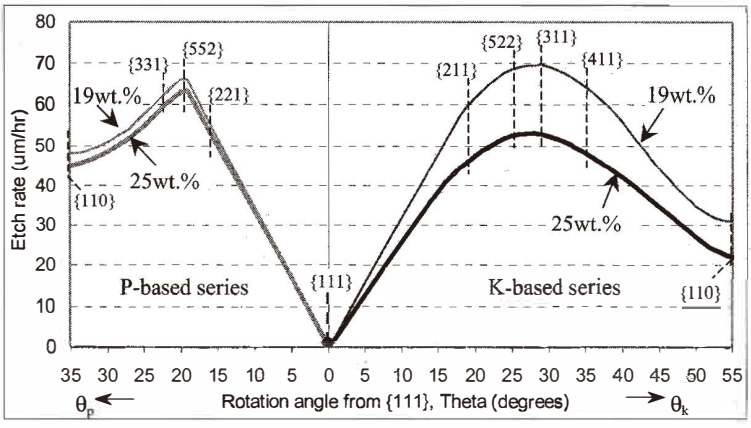

Fig. 9. Estimated canonical P-based and K-based etch rate curves for 25wt.% and 19wt.% TMAH.

†identified as (255), (252), (25$\bar{2}$), (25$\bar{5}$)

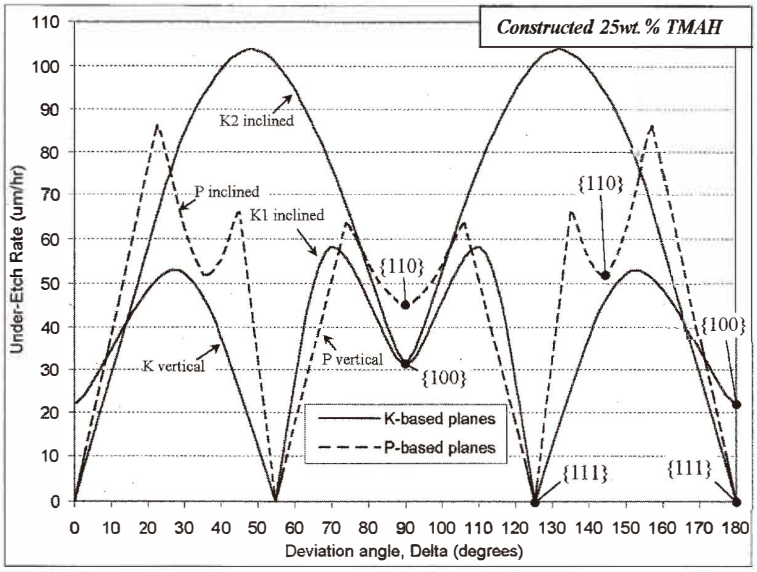

Fig. 10(a). Constructed under-etch rates (from Fig. 9, 25wt% curves) of P-based and K-based planes in Si{110} etched in 25wt.% TMAH.

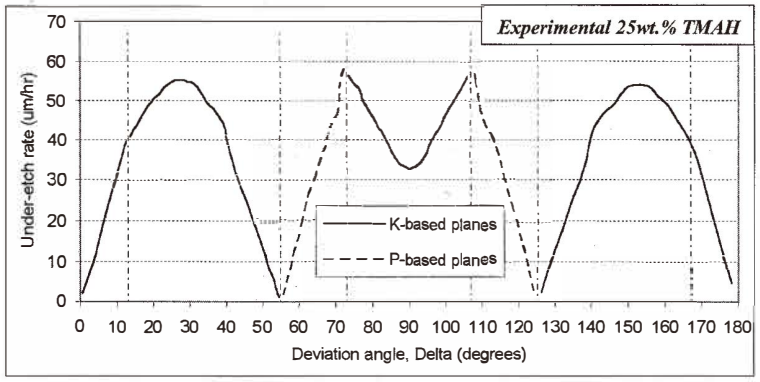

Fig. 10(b). Experimental under-etch rate in Si{110}, 25wt.% TMAH.

3.4 *Under-etch profile predictions*

Based on the canonical curves in Fig. 9, one can also predict the under-etch profile characteristics, such as the number, size, and inclination angles of the under-etched facets. Figure 11 shows examples of predicted under-etch profiles for Si{100} etched in 25wt.% and 19wt.% TMAH.

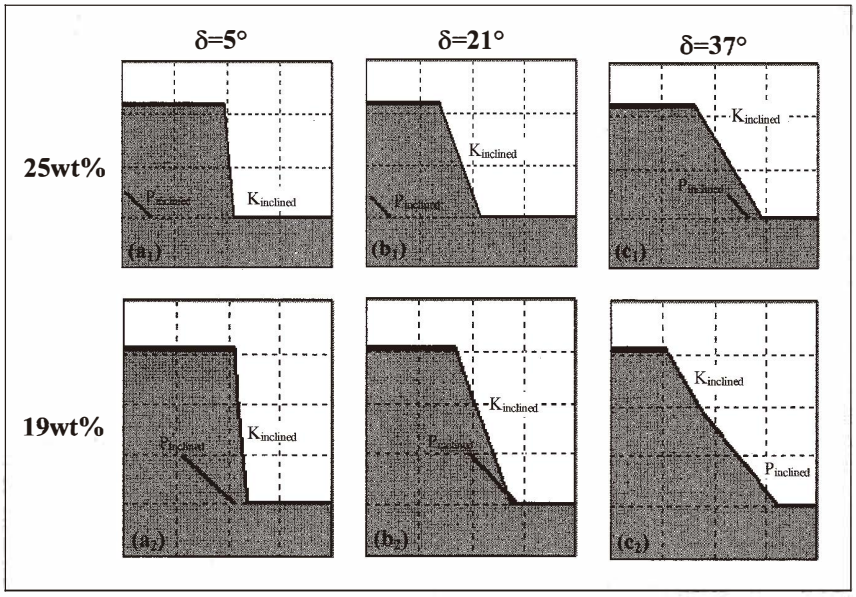

Fig. 11. Si{100} predicted under-etch profiles (based on the canonical curves in Fig. 9) for δ=5°, δ=21° and δ=37°, for 25wt% and 19wt% TMAH.

4. Under-Etch Anomalies

The model described above assumes that all under-etching facets are P-based or K-based. It then becomes possible to identify planes of the same Miller index family that are in different configurations (different inclination angles with different adjacent planes). For the model to ideally apply, the etch rates of these same-index planes should be identical regardless of the configuration. However, this hypothesis is contradicted by some interesting observations presented below. The deviations are suggested to be due to boundary effects occurring at junctions between facets.

4.1 *Etching of PBCs and K-rows*

PBCs and K-rows (which define P-based and K-based facets) are chains of atoms hypothesized to be etched by the removal ("nucleation") of one atom of the chain or row, then by propagation to adjacent atoms (a "zipping" process). One possibility for interaction between facets is through the propagation of zipping chains or rows across a facet boundary. Through that process, facets may "interact," potentially modifying their etch rate. For example, Fig. 12 and Fig. 13 show two inclined K-based facets (labelled K1 and K2) on which the orientation of K-rows is clearly seen. These two facets are suspected to be interacting.

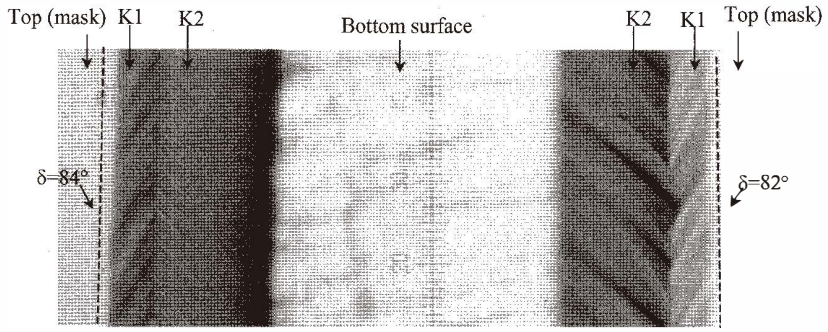

Fig. 12. Top-view micrograph of the K-based inclined under-etch facets at δ=82° and δ=84° on Si{110} etched for 5 h in 25wt.% TMAH.

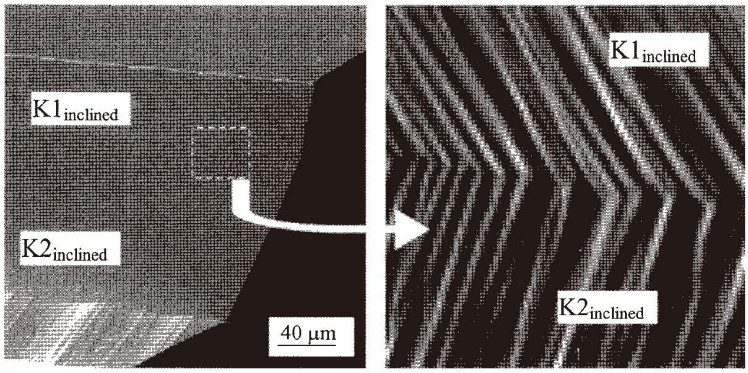

Fig. 13. (a) SEM side views of K1 and K2 inclined planes at δ=84° on Si{110} etched for 5 h in 25wt.% TMAH. (b) Magnification of the junction between K1 and K2 showing the orientation of the K-rows on the facets and a possible interaction between these K-rows.

4.2 *Inverted planes*

An inverted plane is defined as having an inclination angle (α_{inv}) greater than 90°. Such a plane can only be the first (top-most) facet of an under-etched surface. For most cases, the second facet is found to be a symmetrically-inclined ($\alpha = 180 - \alpha_{inv}$) facet of the same Miller Index family. Figure 14 demonstrates that inverted planes are etched more slowly than inclined ones. The existence of inverted planes clearly shows that the same crystal features, in close proximity to each other, are etched at different rates.

The growth of an inverted plane must be due to its etch rate being slow relative to that of its noninverted partner. This may be due to its smaller size, making its etch rate potentially more influenced by its boundaries. In this case, one may hypothesize that the boundary between a pair of same-index family planes may block propagation (zipping of PBCs or K-rows) across the facet boundary.

Figure 15 shows SEM micrographs at $\delta = 37.2°$ for Si{100} 25wt.% TMAH. It is

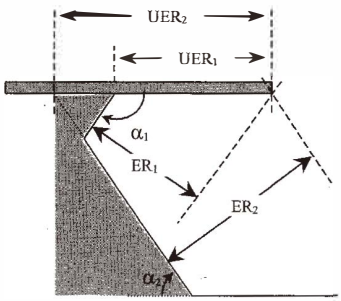

$$ER_2 = UER_2 \sin(\alpha_2)$$

$$ER_1 = UER_1 \sin(\alpha_1)$$
$$= UER_1 \sin(\pi-\alpha_2)$$
$$= UER_1 \sin(\alpha_2)$$

$$UER_1 < UER_2 \rightarrow ER_1 < ER_2$$

Fig. 14. Etch rates of inverted and inclined planes.[16]

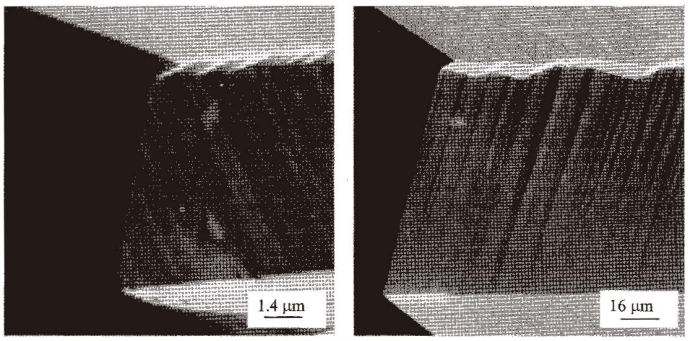

(a) 25 min **(b) 5h**

Fig. 15. Under-etch profiles at deviation angle $\delta \approx 37.2°$ in Si{100} 25wt%.

observed that the inverted and inclined planes have constant relative size with time (from 25 min to 5 h etching), indicating that at this etchant concentration, the inverted and inclined planes have different but constant etch rates.

4.3 *UER variations with time*

Etch rate acceleration or deceleration can be identified by inspecting the evolution with time of the UER curves. For example, Fig. 16 shows clear acceleration of the UER in the range of $\delta = 30°–40°$ on Si{110} in 19wt.% TMAH. Note that each of these curves represents the overall under-etch rate of the top-most facet up to that time (not the instantaneous under-etch rate).

SEM micrographs in Fig. 17 show the evolution of the corresponding facet morphologies at $\delta = 32°$. At 25 min, only a pair of same-index P-based facets are present (one of them inverted). This corresponds to a slow etch rate, consistent with the facet boundary being "blocked". At 1 h 30 min, a new facet, $K2_{inclined}$, emerges, and, simultaneously, the other already-existing facets appear to accelerate. Note that, at 5 h, the size of the $K2_{inclined}$ facet has increased substantially, indicating that other facets are being etched relatively faster.

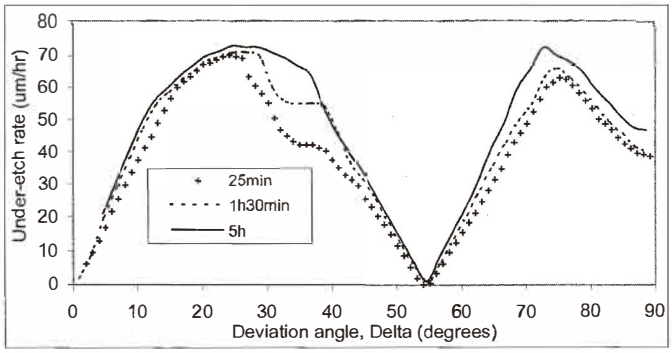

Fig. 16. Si{110} experimental under-etch rate curve evolution with time in 19wt.% TMAH.

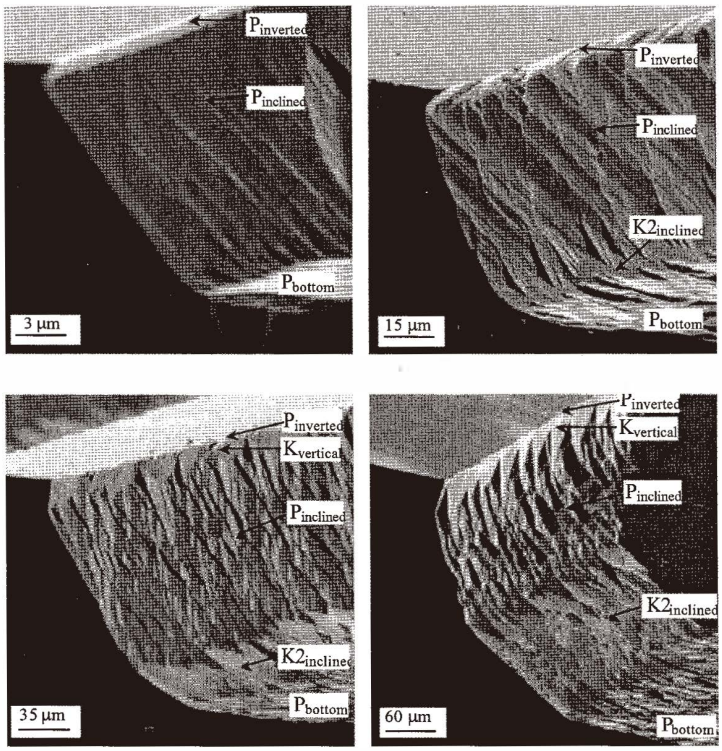

Fig. 17. SEM perspective views showing the size and roughness evolution with time of the under-etch facets at δ=32° on Si{110} 19wt.% TMAH.

Figure 18 shows a reconstructed profile corresponding to the under-etch situation of Fig. 17. Comparison of Fig. 18 with Fig. 17(c) suggests that the $P_{inclined}$ facet at 3 h should have etched faster than predicted to enable the apparition of $K_{vertical}$ and $K2_{inclined}$ facets.

In contrast, for Si{100}, the UER curve experiences a decrease with time (shown in Fig. 19 in the range of $\delta = 15°–27°$). SEM views at $\delta = 22°$ (Fig. 20), show evolution from a very rough inverted "facet" to more-vertical features (still very rough).

4.4 *Interactions with the bottom surface*

The bottom surfaces of the etched wagon-wheel cavities are also free to interact with adjacent inclined facets. Figure 21 shows etch rates measured at the edges of the {110} bottom surfaces after 50 min and 3 h in 19wt.% TMAH.

The two curves in Fig. 21 exhibit similar variation with δ, but the etch rate is greater at the longer time. The etch rate variations with respect to δ may be influenced by interactions of the {110} plane with the bottom-most facet of the under-etched surfaces. Using SEM, the bottom-most facet was identified to be the $K2_{inclined}$ facet (Fig. 22), except for in the

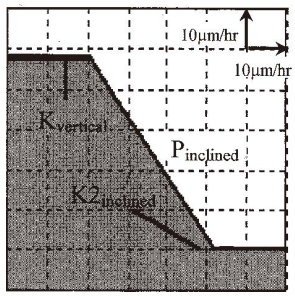

Fig. 18. Under-etch profile at δ=32° constructed from the canonical curves (19wt.%) of Fig. 9.

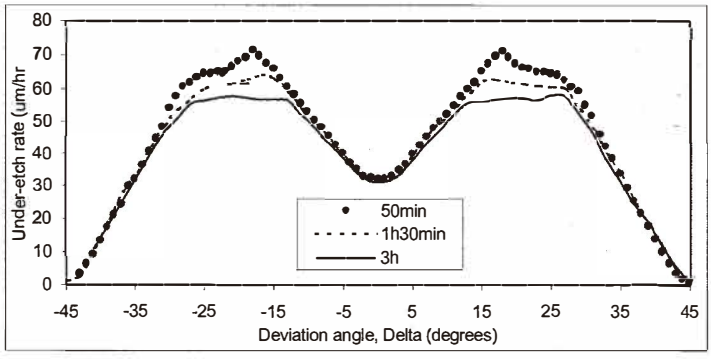

Fig. 19. Si{100} experimental under-etch rate curve evolution with time in 19wt.% TMAH.

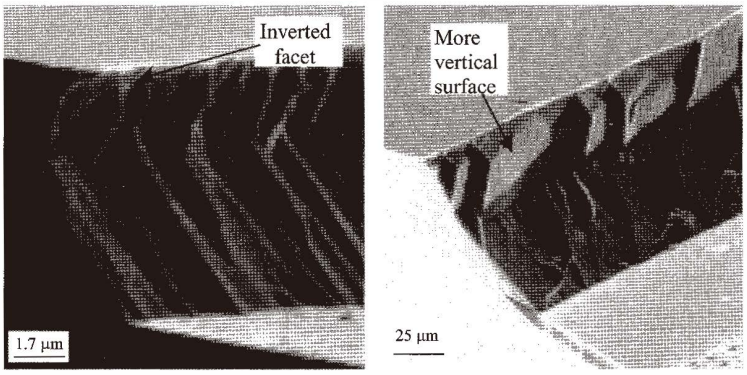

Fig. 20. SEM perspective views at δ=21° showing the near vertical plane which experiences an etch rate deceleration in Si{100} 19wt%.

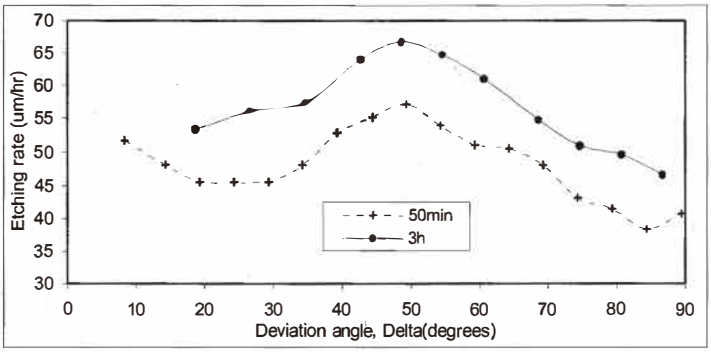

Fig. 21. {110} etching rates measured at the edges of the bottom surfaces in 19wt.% TMAH.

range of δ around 54.74° where only a vertical {111} facet is present. As a result, one may suggest the hypothesis that the $K2_{inclined}$ facet may be responsible for accelerating the {110} surface at the bottom of the cavity. To test this hypothesis, the etch rates of the $K2_{inclined}$ (imported from the K-based 25wt.% canonical curve of Fig. 9) and the {110} bottom surface (experimental) are plotted in the same graph for 25wt% in Fig. 23. A clear correlation is observed in Fig. 23 between the etch rate of $K2_{inclined}$ and the etch rate of the edge of the cavity bottom.

The interactions, which appear to be originating at the junction between inclined planes and the bottom surface, may explain the presence of trenches on the {110} bottom surface. These trenches propagate over time toward the center of the cavity (shown in Fig. 24). The roughness visible in the trenches is aligned parallel to the direction of the PBCs on the {110} surfaces. As shown in Figs. 24(a)–(c), after some hours of etching, these trenches meet at the center of the cavity.

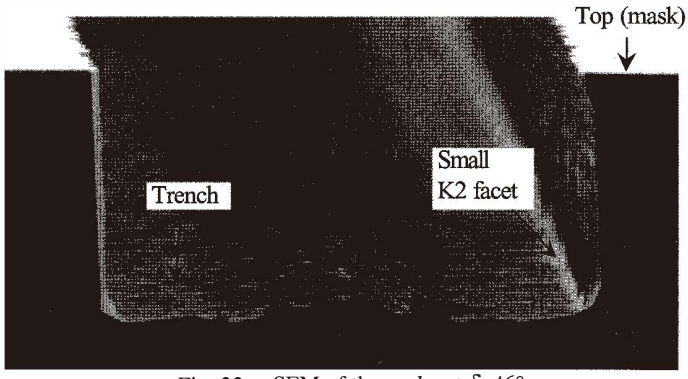

Fig. 22. SEM of the spoke at δ=46°.

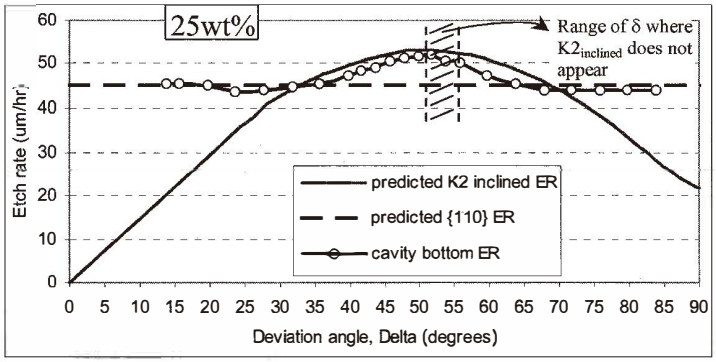

Fig. 23. Etching rate correlation between $K2_{inclined}$ facet and the cavity bottom surface as a function of δ in 25wt.% TMAH. The predicted curves are obtained using the canonical (25wt.%) curves of Fig. 9.

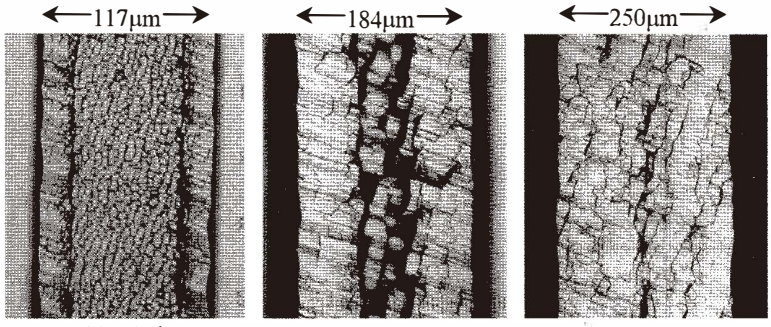

Fig. 24. Top-view micrographs showing trench evolution with time at δ=70° on Si{110} etched in 19wt.% TMAH.

5. Conclusion

Most under-etched surface facets are defined by either PBCs or kink-rows. Indeed, the shapes of under-etch curves can be understood based on this assumption. However, same-index planes are not always etched at the same rates. The differences may be due to interactions between facets, operating at or through the boundaries of the facets. Altered facet etch rates, inverted facets, the formation of trenches, and etch depth variations may all be partly explained by facet boundary effects.

Acknowledgement

This work was partially supported by funding from the Natural Sciences and Engineering Research Council of Canada (NSERC).

References

1 A. Pandy, L. M. Landsberger and M. Kahrizi: Can. J. Elec. & Comp. Eng. **25** (2000) 19.
2 H. Seidel, L. Csepregi, A. Heuberger and H. Baumgartel: J. Electrochem. Soc. **137** (1990) 3612.
3 D. L. Kendall: J.Vac. Sci. & Technol. A **8** (1990) 3598.
4 O. Tabata, R. Asahi, H. Funabashi, K. Shimaoka and S. Sugiyama: *S*ensors and Actuators A **34** (1992) 51.
5 A. Merlos, M. Acero, M. H. Bao, J. Bausells and J. Steve: Sensors and Actuators A **37-38** (1993) 737.
6 M. Elwenspoek, U. Lindberg, H. Kok and L. Smith: Proc IEEE-MEMS-1994 (Oiso, Japan, 1994) p. 223.
7 S. S. Tan, M. L. Reed, H. Han and R. Boudreau: J. Microelectromech. Sys. **5** (1996) 66.
8 L. M. Landsberger, S. Naseh, M. Kahrizi and M. Paranjape: J. Microelectromech. Sys. **5** (1996) 106.
9 O. Tabata: Proc. IEEE-MEMS-1998 (Heidelberg, Germany, 1998) p. 229.
10 K. Sato, M. Shikida, T. Yamasiro, M. Tsunekawa and S. Ito: Proc. IEEE-MEMS 1998, (Heidelberg, Germany, 1998) p. 201.
11 M. Sekimura: Proc. IEEE-MEMS-1999 (Orlando, USA, 1999) p.650.
12 J. van Suchtelen, K. Sato, E. van Veenendaal, A. J. Nijdam, J. G. E. Gardeniers, W. J. P. van Enckevort and M. Elwenspoek: Proc. IEEE-MEMS-1999 (Orlando, USA, 1999) p. 332.
13 L. M. Landsberger, A. Pandy and M. Kahrizi: Sensors and Materials 13 (2001) 293.
14 R. A. Wind and M. A. Hines:Surf. Sci. 460, 21 (2000).
15 A. J. Nijdam, J. W. Berenschot, J. van Suchtelen, J.G.E. Gardeniers and M. Elwenspoek: J. Micromech.Microeng **9** (1999)135.
16 Z. Elalamy, L. M. Landsberger, A. Pandy, M. Kahrizi, I. Stateikina and S. Michel: Journal of Vacuum Science and Technology A **20** (2002) 1927.
17 Z. Elalamy: "Modelling of Anisotropic Etching of Silicon in TMAH: Anomalies due to Facet Boundary Effects," Master of Applied Science Thesis in the Department of Electrical and Computer Engineering, Concordia University, Montreal, Canada (2002).
18 A. Pandy: "Experimental Investigations of Anisotropic Etching of Silicon," Master of Applied Science Thesis in the Department of Electrical and Computer Engineering, Concordia University, Montreal, Canada (2002).
19 J. G. E. Gardeniers, W. E. J. R Maas, R. Z. C. Van Meerten and L. J. Gilling: J. Cryst. Growth **96** (1989) 832.